导读Aggressive Flight With Suspended Payloads Using Vision-Based Control

0.Abstract

本文使用下视摄像头观察并估计负载，实现了负载三维空间的闭环控制，规划，估计。能够实现负载最大垂直于地面53°的控制，首次实现了大角度悬挂负载的闭环敏捷策略

1.Introduction

过去的相关工作都通过限制运动维度，将三维运动压缩为二维（平面）进行的控制，完全依赖于外部运动捕捉系统和无人机的闭环控制而不是对负载的位置控制。

2.建模

TABLE I
VARIABLES OF THE QUADROTOR-WITH-LOAD SYSTEM

$\mathcal{I}, \mathcal{B}, \mathcal{C}$	Inertial, body, camera frame
$l, d \in \mathbb{R}$	Cable length, distance from camera to load
$m_Q, m_L; g \in \mathbb{R}$	Mass of quad, load; gravity constant
$\mathbb{I} \in \mathbb{R}^{3,3}$	Inertia tensor of quad, in $\mathcal{B}$
$f \in \mathbb{R}, \mathbf{M} \in \mathbb{R}^3$	Input thrust magnitude, moment in $\mathcal{B}$
$\mathbf{x}_Q, \mathbf{x}_L \in \mathbb{R}^3$	Position vector of quad, load, in $\mathcal{I}$
$\mathbf{p} \in \mathbb{S}^2$	Unit vector from quad to load, in $\mathcal{I}$
$\mathbf{R} \in SO(3), \psi \in \mathbb{R}$	Rotation from $\mathcal{B}$ to $\mathcal{I}$, yaw angle of quad
$\mathbf{\Omega} \in \mathbb{R}^3$	Angular velocity of quad, in $\mathcal{B}$

假设负载为一质量点，绳子为无质量的棒

$\mathcal{I}$

a massless rod. Let $\mathcal{I}$ be an inertial coordinate frame, with axes $\{\mathbf{e}_x^{\mathcal{I}}, \mathbf{e}_y^{\mathcal{I}}, \mathbf{e}_z^{\mathcal{I}}\}$, $\mathcal{B}$ be a body frame with axes $\mathbf{e}_*^{\mathcal{B}}$, and $\mathcal{C}$ be a camera frame with axes $\mathbf{e}_*^{\mathcal{C}}$. Fig. 2 illustrates these frames and

Table I lists relevant variables. The state and input are:

$$\mathbf{x} = \begin{bmatrix} \mathbf{x}_L^\top \ \dot{\mathbf{x}}_L^\top \ \mathbf{p}^\top \ \dot{\mathbf{p}}^\top \ \mathbf{R} \ \boldsymbol{\Omega}^\top \end{bmatrix}^\top,$$

$$\mathbf{u} = \begin{bmatrix} f \ \mathbf{M}^\top \end{bmatrix}^\top,$$

respectively. $\mathbf{p}$ and $\mathbf{R}$ are coordinate-free configuration representations that avoid parameterization singularities.

系统动能和势能

$\mathcal{T} = \frac{1}{2}(m_Q + m_L)\dot{\mathbf{x_L}} \cdot \dot{\mathbf{x_L}} - m_Q l \dot{\mathbf{x_L}} \cdot \dot{\mathbf{p}}$
$+ \frac{1}{2} m_Q l^2 \dot{\mathbf{p}} \cdot \dot{\mathbf{p}} + \frac{1}{2} \Omega \mathbb{I} \Omega$

$$\mathcal{U} = (m_Q + m_L) g \, \mathbf{x}_L \cdot \mathbf{e}_z^{\mathcal{I}} - m_Q g l \, \mathbf{p} \cdot \mathbf{e}_3,$$

虚拟功

$$\delta \mathcal{W} = f \boldsymbol{R} \mathbf{e}_z^{\mathcal{I}} \cdot (\delta \mathbf{x}_L - l \delta \mathbf{p}) + \mathbf{M} \cdot (\boldsymbol{R}^\top \delta \boldsymbol{R}).$$

偏差

The variation $\delta \mathbf{x}_L$ exists in $\mathbb{R}^3$, however, the other variational terms must be defined on their respective manifolds:

$$\delta \mathbf{p} = \hat{\boldsymbol{\xi}} \mathbf{p} \in T\mathbb{S}^2, \boldsymbol{\xi} \in \mathbb{R}^3, \text{ where } \boldsymbol{\xi} \cdot \mathbf{p} = 0,$$

$$\delta \mathbf{R} = \mathbf{R} \hat{\boldsymbol{\eta}} \in TSO(3), \boldsymbol{\eta} \in \mathbb{R}^3.$$

The hat map, $\hat{\cdot}$, returns the skew-symmetric matrix such that $\hat{\mathbf{x}}\mathbf{y} = \mathbf{x} \times \mathbf{y}$. $\delta \dot{\mathbf{x}}_L, \delta \dot{\mathbf{p}}, \delta \boldsymbol{\Omega}$ can be found by differentiation. Us-

Lagrange-d'Alembert型可积的微分方程

$$\delta S = \int_{t_1}^{t_2} (\delta W + \delta \mathcal{T} - \delta \mathcal{U}) dt = 0,$$

and integrating by parts gives the system dynamics:

$$\begin{aligned}
\tfrac{d}{dt}\mathbf{x}_L &= \dot{\mathbf{x}}_L, \\
(m_Q + m_L)(\ddot{\mathbf{x}}_L + g\mathbf{e}_z^{\mathcal{I}}) &= \left(\mathbf{p} \cdot f\mathbf{R}\mathbf{e}_z^{\mathcal{I}} - m_Q l\left(\dot{\mathbf{p}} \cdot \dot{\mathbf{p}}\right)\right)\mathbf{p}, \\
\tfrac{d}{dt}\mathbf{p} &= \dot{\mathbf{p}}, \\
m_Q l\left(\ddot{\mathbf{p}} + \left(\dot{\mathbf{p}} \cdot \dot{\mathbf{p}}\right)\mathbf{p}\right) &= \mathbf{p} \times \left(\mathbf{p} \times f\mathbf{R}\mathbf{e}_z^{\mathcal{I}}\right), \\
\dot{\mathbf{R}} &= \mathbf{R}\,\hat{\boldsymbol{\Omega}}, \\
\dot{\boldsymbol{\Omega}} &= \mathbb{I}^{-1}\left(\mathbf{M} - \boldsymbol{\Omega} \times \mathbb{I}\,\boldsymbol{\Omega}\right).
\end{aligned}$$

Details of this calculation can be found in [12].

K. Sreenath, T. Lee, and V. Kumar, “Geometric control and differential flatness of a quadrotor UAV with a cable-suspended load,” in Proc. IEEE Conf. Decis. Control, Dec. 2013, pp. 2269–2274.

系统关键还是differentially flat，将状态和输入表示为一组变量（x,y,z,yaw)及其导数的非线性方程

, the flat variables are [12]:

$$\mathbf{x}_f = \left[\mathbf{x}_L^\top \ \psi\right]^\top.$$

对负载也做于无人机相应的变量压缩处理，这里的yaw仍然是无人机的yaw，对负载的姿态可以忽略

To see this, begin with the Newton-Euler equation:

$$-T\mathbf{p} = m_L(\ddot{\mathbf{x}}_L + g\mathbf{e}_z^{\mathcal{I}}), \tag{1}$$

where T represents the magnitude of the cable tension. Then:

$$\mathbf{p} = -\frac{\left(\ddot{\mathbf{x}}_L + g\mathbf{e}_z^{\mathcal{I}}\right)}{\|\ddot{\mathbf{x}}_L + g\mathbf{e}_z^{\mathcal{I}}\|_2}, \tag{2}$$

$\dot{\mathbf{p}}$ can be found through differentiation of (2). The quadrotor's position and higher derivatives can then be found using:

$$\mathbf{x}_Q = \mathbf{x}_L - l\mathbf{p}. \tag{3}$$

The quadrotor is a differentially-flat system with flat variables $\left[\mathbf{x}_Q^\top \ \psi\right]^\top$ [19], so the rotational states and input can be derived. The highest derivatives of $\mathbf{x}_L$, ψ needed to recover $\mathbf{x}$ and $\mathbf{u}$ are $\mathbf{x}_L^{(6)}$, $\ddot{\psi}$, respectively. For the remainder of this work, assume ψ is constant. Furthermore, assume the cable remains taut (i.e., $T > 0$). From (1), this is ensured for $\|\ddot{\mathbf{x}}_L + g\mathbf{e}_z^{\mathcal{I}}\|_2 > 0$, which we will guarantee during planning.

利用负载的状态反推无人机状态。论文中假设yaw是不变的，绳子一直都是拉紧的，即负载一直都是受无人机控制的

3.控制

重中之重：跟踪轨迹

des 表示规划的轨迹

c 表示控制器计算得到的控制指令

Differential flatness（微分平坦），保证了负载规划轨迹$\mathbf{X_{L,des}}$的任意六阶可以被映射到无人机的动力学状态$\mathbf{X_{des}}$和输入$\mathbf{u_{des}}$。因此轨迹的优化可以直接根据负载的期望状态进行，SectionV的内容

采用分层控制，如图

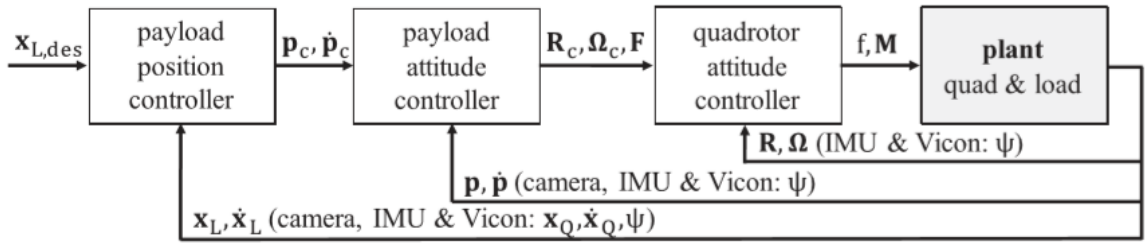

Fig. 3. Controller structure and sensor feedback.

期望负载轨迹直接输入**负载位置控制器**获得**期望负载姿态和角速度**，**负载姿态控制器**结合实际姿态和角速度计算的**无人机期望姿态，角速度和升力**，**无人机姿态控制器**计算的最终输入**升力和力矩**

为了实现大角度摆动控制，因此无法进行线性化处理（小角度假设）或姿态参数化（奇异性）

无人机姿态控制器(P)

c 表示控制器计算得到的控制指令

$$\begin{aligned}\mathbf{M} = & -\mathbf{k}_R\mathbf{e}_R - \mathbf{k}_\Omega\mathbf{e}_\Omega \\ & + \boldsymbol{\Omega}\times\mathbb{I}\boldsymbol{\Omega} - \mathbb{I}\left(\hat{\Omega}\times\mathbf{R}^\top\mathbf{R}_c\boldsymbol{\Omega}_{\boldsymbol{c}} - \mathbf{R}^\top\mathbf{R}_c\dot{\boldsymbol{\Omega}}_c\right),\end{aligned}$$

with error functions:

$$\mathbf{e}_R = \tfrac{1}{2}\left(\mathbf{R}_c^\top\mathbf{R} - \mathbf{R}^\top\mathbf{R}_c\right)^\vee,\ \mathbf{e}_\Omega = \boldsymbol{\Omega} - \mathbf{R}^\top\mathbf{R}_c\boldsymbol{\Omega}_c,$$

where $(\cdot)^\vee$ is the inverse of the hat map and $\mathbf{k}_R, \mathbf{k}_\Omega$ are diagonal gain matrices. Unlike a linearized controller, the error functions are defined on the manifold $TSO(3)$. For positive-definite gain matrices and initial conditions where the angle-axis rotation from $\mathbf{R}$ to $\mathbf{R}_c$ has angle less than $180°$, the closed-loop quadrotor attitude error dynamics are exponentially stable about $(\mathbf{e}_R, \mathbf{e}_\Omega) = \mathbf{0}$ [12], [20].

负载姿态控制器(PD)

$\mathbf{R}_c, \boldsymbol{\Omega}_c$, are obtained from the payload attitude controller:

$$\begin{aligned}\mathbf{F} = m_Q l\big(&-k_p\mathbf{e}_p - k_{\dot{p}}\mathbf{e}_{\dot{p}} + \left(\mathbf{p}\cdot(\mathbf{p}_c\times\dot{\mathbf{p}}_c)\right)(\mathbf{p}\times\dot{\mathbf{p}}) \\ &+ (\mathbf{p}_c\times\ddot{\mathbf{p}}_c)\times\mathbf{p}\big) - (\mathbf{p}_c\cdot\mathbf{p})\mathbf{p}_c. \qquad (4)\end{aligned}$$

$\mathbf{F}$ is defined with error functions:

$$\mathbf{e}_p = \hat{\mathbf{p}}^2\mathbf{p}_c,\ \ \mathbf{e}_{\dot{p}} = \dot{\mathbf{p}} - (\mathbf{p}_c\times\dot{\mathbf{p}}_c)\times\mathbf{p}.$$

Again, $\mathbf{e}_p, \mathbf{e}_{\dot{p}}$ are defined directly on the manifold $T\mathbb{S}^2$. From (4), the thrust input can be found as:

$$f = \mathbf{F} \cdot \mathbf{R}\mathbf{e}_z^{\mathcal{I}}.$$

The commanded orientation is found as:

$$\mathbf{R}_c = \left[\frac{\mathbf{b}_{3c} \times \mathbf{c}_{1c}}{\|\mathbf{b}_{3c} \times \mathbf{c}_{1c}\|_2} \times \mathbf{b}_{3c} \;\; \frac{\mathbf{b}_{3c} \times \mathbf{c}_{1c}}{\|\mathbf{b}_{3c} \times \mathbf{c}_{1c}\|_2} \;\; \mathbf{b}_{3c} \right], \hat{\Omega}_c = \boldsymbol{R}_c^\top \dot{\boldsymbol{R}}_c, \quad (5)$$

where:

$$\mathbf{b}_{3c} = \frac{\mathbf{F}}{\|\mathbf{F}\|_2}, \; \mathbf{c}_{1c} = \begin{bmatrix} \cos(\psi) & \sin(\psi) & 0 \end{bmatrix}^\top.$$

$\dot{\mathbf{R}}_c$ and $\dot{\mathbf{\Omega}}_c$ can be found by differentiating (5). For positive gains $k_p, k_{\dot{p}}$ and initial angles less than 180° between $\mathbf{p}$ and $\mathbf{p}_c$, the state $(\mathbf{e}_p, \mathbf{e}_{\dot{p}}, \mathbf{e}_R, \mathbf{e}_\Omega) = \mathbf{0}$ is an exponentially stable equilibrium of the closed-loop error dynamics [12].

c_{1c} 计算的中间坐标系

负载位置控制器（PID)

Finally, the payload position controller is:

$$\mathbf{A} = (m_Q + m_L) \left(-\mathbf{k}_x \mathbf{e}_{x_L} - \mathbf{k}_v \mathbf{e}_{\dot{x}_L} - \mathbf{k}_i - \int \mathbf{e}_{x_L} dt \right)$$
$$+ (m_Q + m_L)(\ddot{\mathbf{x}}_L + g\mathbf{e}_z^{\mathcal{I}}) + m_Q l(\dot{\mathbf{p}} \cdot \dot{\mathbf{p}})\mathbf{p},$$

where $\mathbf{k}_x, \mathbf{k}_v, \mathbf{k}_i$ are diagonal gain matrices, $\mathbf{e}_{x_L} = \mathbf{x}_L - \mathbf{x}_{L,des}$, and $\mathbf{e}_{\dot{x}_L} = \dot{\mathbf{x}}_L - \dot{\mathbf{x}}_{L,des}$. This defines a commanded payload orientation:

$$\mathbf{p}_c = -\frac{\mathbf{A}}{\|\mathbf{A}\|_2}.$$

$\dot{\mathbf{p}}_c$ can again be found through direct differentiation. For positive-definite $\mathbf{k}_x, \mathbf{k}_v, \mathbf{k}_i$ and initial payload and quadrotor attitude errors satisfying the previously stated bounds, the complete closed-loop error dynamics are exponentially attractive about $(\mathbf{e}_x, \mathbf{e}_y, \mathbf{e}_p, \mathbf{e}_{\dot{p}}, \mathbf{e}_R, \mathbf{e}_\Omega) = \mathbf{0}$ [12].

4.负载估计

算法：ExtendedKalmanFilter(EKF),yielding high-frequency,dynamics-informedestimates

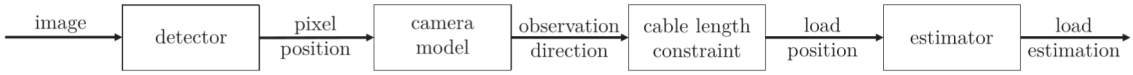

Fig. 4. Flow diagram of the payload estimation pipeline.

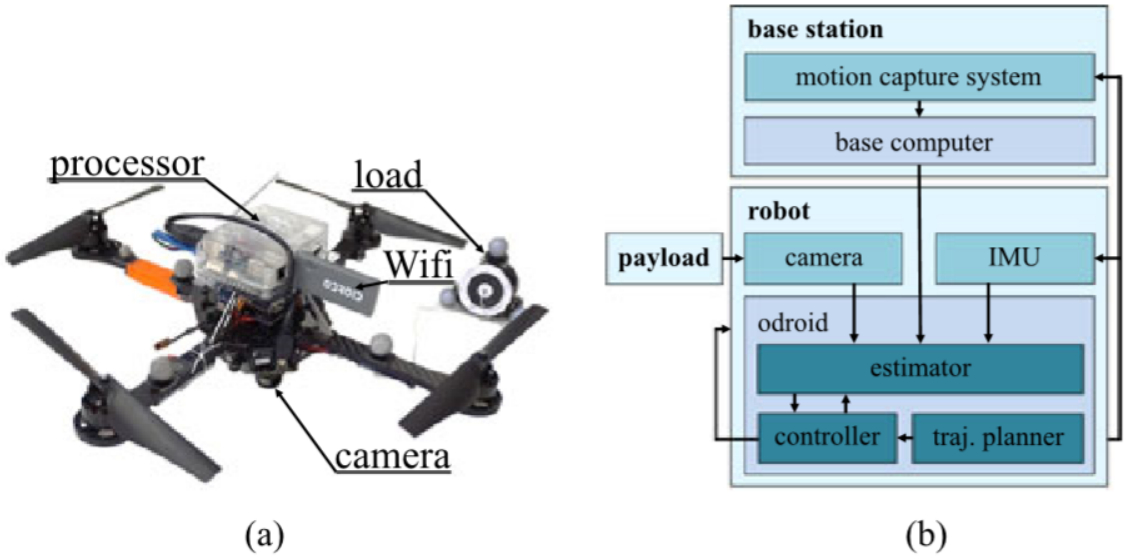

Fig. 5. Overview of experimental setup. (a) Hardware components. (b) Experimental architecture.

A. Detector

开源的检测器

`T. Krajn´ık et al., “A practical multirobot localization system,” J. Intell. Robot. Syst., vol. 76, pp. 539–562, 2014`

黑白相间圆得到亚像素精度的像素位置

$$\mathbf{x}_u = [u, v]^\top$$

B. 相机模型

获取负载到相机的单位向量**n^C**

We model the camera with an omnidirectional model [22]. An affine transformation between the tag center in pixel coordinates,

$\mathbf{x}_u = [u, v]^\top$, and adjusted pixel coordinates, $\mathbf{x}_{u'} = [u', v']^\top$, accounting for lens-sensor misalignments. The vector from the camera to payload, in the camera frame, is:

$$\mathbf{n}^{\mathcal{C}} = \begin{bmatrix} n_x \\ n_y \\ n_z \end{bmatrix} \approx \lambda \begin{bmatrix} u' \\ v' \\ f(u', v') \end{bmatrix},$$

where the factor λ accounts for the scale ambiguity. The imaging function $f(u', v')$ is approximated with a Taylor series expansion. Assuming the lens is rotationally symmetric, we define $\rho := \sqrt{u'^2 + v'^2}$ and express the Taylor series as:

$$f(u', v') = f(\rho) = a_0 + a_1\rho + a_2\rho^2 + \ldots + a_N\rho^N, \quad (6)$$

where N is tuned. The affine transformation and $a_0, \ldots, a_N$ are found during calibration. This allows us to obtain $\mathbf{n}^{\mathcal{C}}$.

C. 绳长约束

得到负载相对于无人机的位置

From Fig. 2, we see under the cable-taut assumption that:

$$\mathbf{x}_L^{\mathcal{B}} = l\,\mathbf{p}^{\mathcal{B}} = \mathbf{x}_C^{\mathcal{B}} + d\,\mathbf{R}_{\mathcal{C}}^{\mathcal{B}}\,\mathbf{n}^{\mathcal{C}}. \quad (7)$$

$\mathbf{x}_L^{\mathcal{B}}$ is payload's position and $\mathbf{x}_{\mathcal{C}}^{\mathcal{B}}$ is the camera's position, both in the body frame. $\mathbf{R}_C^{\mathcal{B}}$ is the camera-to-body-frame rotation matrix. Also, note that $\mathbf{x}_{\mathcal{C}}^{\mathcal{B}}$ is known. We formulate:

$$l = \left|\mathbf{x}_C^{\mathcal{B}} + d\,\mathbf{n}^{\mathcal{B}}\right|,$$

and solve for d. We select the solution corresponding to the load oriented below the quadrotor. We then use (7) to find $\mathbf{x}_L^{\mathcal{B}}$, the position of the payload relative to the quadrotor.

D. 基于模型的估计器

For estimation, we consider a system with state:

$$\mathbf{X} = \begin{bmatrix} \mathbf{p}^\top & \dot{\mathbf{p}}^\top \end{bmatrix}^\top,$$

where $\mathbf{p}, \dot{\mathbf{p}}$ are in $\mathcal{I}$, with input:

$$\mathbf{U} = \begin{bmatrix} f & \boldsymbol{R} & \boldsymbol{\Omega}^\top \end{bmatrix}^\top.$$

Here, f is calculated by the controller while $\mathbf{R}$ and $\boldsymbol{\Omega}$ are obtained from IMU and Vicon yaw measurements.

We model the process noise as additive Gaussian white noise $\mathbf{N} \in \mathbb{R}^6$ with zero mean and standard deviation $\mathbf{Q} \in \mathbb{R}^{6,6}$. The resulting process model is:

$$\begin{aligned} \dot{\mathbf{X}} &= \begin{bmatrix} \dot{\mathbf{p}} \\ \ddot{\mathbf{p}} \end{bmatrix} = \mathbf{f}(\mathbf{X}, \mathbf{U}, \mathbf{N}), \quad \mathbf{N} \sim \mathcal{N}(0, \mathbf{Q}), \\ &= \begin{bmatrix} \dot{\mathbf{p}} \\ \frac{1}{m_Q l}\mathbf{p} \times (\mathbf{p} \times f\mathbf{R}\mathbf{e_3}) - (\dot{\mathbf{p}} \cdot \dot{\mathbf{p}})\mathbf{p} \end{bmatrix} + \mathbf{N}. \end{aligned} \tag{8}$$

We obtain $\mathbf{x}_L^{\mathcal{B}}$ from Sections IV-A–IV-C and calculate a numerical discrete time derivative for $\dot{\mathbf{x}}_L^{\mathcal{B}}$. The measurement model, with additive Gaussian white noise $\mathbf{V} \in \mathbb{R}^6$ with zero mean and standard deviation $\mathbf{S} \in \mathbb{R}^{6,6}$, is:

$$\begin{aligned} \mathbf{Z} &= \begin{bmatrix} \mathbf{x}_L^{\mathcal{B}} \\ \dot{\mathbf{x}}_L^{\mathcal{B}} \end{bmatrix} = \mathbf{g}(\mathbf{X}, \mathbf{U}, \mathbf{V}), \quad \mathbf{V} \sim \mathcal{N}(0, \mathbf{S}), \\ &= \begin{bmatrix} \mathbf{R}^\top l\, \mathbf{p} \\ l\left(\mathbf{R}^\top \dot{\mathbf{p}} - \boldsymbol{\Omega} \times \left(\mathbf{R}^\top \mathbf{p}\right)\right) \end{bmatrix} + \mathbf{V}. \end{aligned} \tag{9}$$

We use Eqs. (8) and (9) in a standard EKF implementation [23]. Note we also formulate the EKF in a coordinate-free manner. While camera measurements are low-frequency, the EKF uses the dynamic model to estimate the state at the higher IMU measurement rate. We conduct a process update when a new IMU measurement is received, using the most recent control input and yaw measurement. When a new raw image is received, we cache the current state estimate, the subsequent IMU and Vicon measurements, and control inputs. After $\mathbf{x}_L^{\mathcal{B}}, \dot{\mathbf{x}}_L^{\mathcal{B}}$ are computed, we conduct the measurement update on the first state

estimate cached and recompute the process updates, accounting for image processing latency.

5. 轨迹规划

核心思想于minimum snap相似，最小化$\mathbf{X}_{\mathbf{L}}^{(6)}$，求解二次规划问题

代价函数

$$\mathbf{x}_{L,des} = \arg\min_{\mathbf{x}_L} \int_0^{t_m} \|\mathbf{x}_L^{(6)}\|_2^2 \, dt. \tag{10}$$

The Euler-Lagrange condition yields the condition:

$$\mathbf{x}_L^{(12)} = 0, \tag{11}$$

whose solution is an 11^{th}-order polynomial. Thus, optimal payload trajectories take the form of piecewise-polynomials:

$$\mathbf{x}_{L,des} = \begin{cases} \mathbf{x}_{L,des,1} = \sum_{i=0}^{11} c_{i,0} t^i & t_0 \le t \le t_1 \\ \mathbf{x}_{L,des,2} = \sum_{i=0}^{11} c_{i,1} t^i & t_1 < t \le t_2 \\ \cdots & \\ \mathbf{x}_{L,des,m} = \sum_{i=0}^{11} c_{i,m-1} t^i & t_{m-1} < t \le t_m, \end{cases}$$

where $\mathcal{T} = \{t_0, ..., t_m\}$ is a pre-selected set of breaktimes and $\mathbf{x}_{L,des}$ is a vector function. Consider the decision vector:

$$\mathbf{c} = \begin{bmatrix} c_{0,0} & c_{1,0} & c_{2,0} & \cdots & c_{N,m-1} \end{bmatrix}^\top.$$

连续性约束

Equation (10) is a positive-definite quadratic function with respect to $\mathbf{c}$. For dynamic feasibility, we impose continuity constraints:

$$\mathbf{x}_{L,des,j}^{(k)}(t_j) = \mathbf{x}_{L,des,j+1}^{(k)}(t_j) \; \forall j \in [0,5], k \in [1, m\text{-}1]. \tag{12}$$

边界约束（始末点中间点位置约束）

To ensure the system begins and ends at hover, we impose:

$$\mathbf{x}_{L,des}^{(k)}(t_j) = \mathbf{0}\ \forall j \in \{0, m\}, k \in [1, 5]. \tag{13}$$

Note that the flat derivatives in (13) correspond to states $\mathbf{p} = -\mathbf{e}_z^{\mathcal{I}},\ \mathbf{R} = \mathcal{I},\ \dot{\mathbf{p}} = \boldsymbol{\Omega} = \mathbf{0}$. Finally, we select waypoints $\mathbf{x}_{L,j}$ for the trajectory to pass through and impose:

$$\mathbf{x}_{L,des}(t_j) = \mathbf{x}_{L,j}\ \forall j \in [0, m]. \tag{14}$$

Equations (12)–(14) are linear with respect to $\mathbf{c}$. Using (10) and (12)–(14), we formulate a Quadratic Program (QP) that can be solved with commercial optimization software [8], [19].

There is a possibility that the optimized trajectory $\mathbf{x}_{L,des}$ violates the cable-tautness assumptions of our system. From (1), guaranteeing $\ddot{\mathbf{x}}_L \cdot \mathbf{e}_z > -g$ is sufficient to ensure $T > 0$. It has been shown that for any $\mathbf{x}_{L,des}$ with breaktimes $\mathcal{T}$, a trajectory with the same coefficients but breaktimes $\alpha\mathcal{T}$ traverses the same path and has derivatives $\frac{\mathbf{x}_{L,des}^{(k)}}{\alpha^k}$ [19]. To ensure cable-tautness, we first find the desired trajectory coefficients by solving the QP with an initial $\mathcal{T}$. We then find the trajectory breaktimes by choosing α such that $\ddot{\mathbf{x}}_L \cdot \mathbf{e}_z > -g$.

这里考虑到规划出来的轨迹可能会导致绳子不是张紧的，因此需要对规划出的轨迹进行处理，通过对时间段乘上一个系数（应该是大于0的）来调整规划的路径保证无人机加速度不至于过大导致无法满足假设。

这里的$\frac{\mathbf{x}_{\mathrm{L,des}}^{(\mathrm{k})}}{\alpha^k}, \alpha = \alpha\tau, \tau = 0, 1$